https://doi.org/10.31436/iiumej.v26i1.3392

# ELECTROCHEMICAL SENSING OF NICOTINE USING LASER-INDUCED GRAPHENE SCREEN PRINTED ELECTRODE

**BALQIS NURNADIA BADROL HISHAM[1], ROSMINAZUIN AB RAHIM[1], ANIS NURASHIKIN NORDIN[1], ALIZA AINI MD RALIB[1], NOR FARAHIDAH ZA'BAH[1], LUN HAO TUNG[2], ZAINIHARYATI MOHD ZAIN[3]**

*[1]Department of Electrical and Computer Engineering, Kulliyyah of Engineering, International Islamic University Malaysia, IIUM, Kuala Lumpur, Malaysia*
*[2]Manufacturing Technology Innovation, Jabil Circuit Sdn. Bhd., Penang, Malaysia*
*[3]Faculty of Applied Science, University Teknologi MARA, UiTM, Selangor, Malaysia*

**Corresponding author: rosmi@iium.edu.my*

*(Received: 5 August 2024; Accepted: 29 August 2024; Published online: 10 January 2025)*

***ABSTRACT:*** Nicotine is one of the major addictive substances in tobacco plants, which caused a global pandemic. Rapid detection of nicotine is crucial to allow quick identification of harmful substances that will cause significant health risks, especially with the recent rise in electronic cigarettes. Since smoking cessation programs are typically limited to screening, awareness, consultation, medication, and follow-up activities, there is a need for a device to check the nicotine level in former smokers at the end of the programs. However, most of the current nicotine detection is based on chromatography technology, which involves complicated sample pre-treatment and bulky and expensive instruments. Thus, screen-printing technology employing electrochemical detection is a promising solution as it offers a simple and portable setup for nicotine detection. Yet, conventional screen-printed electrodes (SPE) have relatively low sensitivity and need modification to improve the electrode material. Therefore, this work aims to investigate the performance of laser-induced graphene (LIG) as SPE-modified electrodes to detect the presence of nicotine through electrochemical measurements. A finite element simulation was conducted to investigate laser power's effect on the induced graphene's quality. The $CO_2$ laser with 3W laser power, Dots per inch (DPI) of 1200, and a laser speed of 13% was used to fabricate the LIG sensor on a Kapton substrate. Material characterizations such as SEM, EDX, and Raman spectra were performed on the fabricated LIG-SPE to confirm the presence of LIG. Cyclic voltammetry (CV) measurement was done using 0.1M $[Fe(CN)_6]^{3-/4-}$ and 0.1M KCL to find the suitable scan rates. At a fixed scan rate of 50 mV/s, the sensor's performance was analyzed using 0.1M of nicotine with 3 different phosphate buffer solutions (PBS) of pH 5, pH 7, and pH 9 at different nicotine concentrations. Nicotine with PBS pH 5 solution was found to be the optimum measured solution, with the value obtained for $R^2$ having the highest value of 0.9988 and the lowest LOD of 4.2183 μM. The proposed electrochemical sensing of nicotine using a laser-induced graphene screen printed electrode can detect nicotine with high linearity at different pH levels of PBS buffer solution.

***ABSTRAK:*** Nikotin adalah salah satu bahan ketagihan utama dalam tumbuhan tembakau yang menyebabkan pandemik global. Pengesanan cepat nikotin adalah penting bagi membolehkan pengecaman cepat bahan merbahaya yang menyebabkan risiko kesihatan ketara terutamanya dengan peningkatan rokok elektronik pada masa sekarang. Memandangkan program berhenti merokok biasanya terhad kepada pemeriksaan, kesedaran, perundingan, ubat-ubatan dan aktiviti susulan, terdapat keperluan bagi peranti memeriksa tahap nikotin dalam bekas perokok pada akhir program. Walau bagaimanapun, kebanyakan

https://doi.org/10.31436/iiumej.v26i1.3392

pengesanan nikotin semasa adalah berdasarkan teknologi kromatografi, di mana melibatkan sampel pra-rawatan rumit, instrumen besar dan mahal. Oleh itu, teknologi percetakan skrin yang menggunakan pengesanan eletrokimia adalah penyelesaian bermakna kerana ia menawarkan persediaan mudah dan mudah alih bagi mengesan nikotin. Namun, skrin-cetakan elektrod konvensional (SPE) mempunyai sensitiviti rendah dan memerlukan pengubahsuaian bagi menambah baik bahan elektrod. Oleh itu, kajian ini adalah untuk menyiasat prestasi laser graphen teraruh (LIG) sebagai elektrod SPE yang diubah suai bagi mengesan kehadiran nikotin melalui pengukuran elektrokimia. Simulasi unsur terhingga telah dijalankan bagi melihat kesan kuasa laser ke atas kualiti graphen teraruh. Laser $CO_2$ dengan kuasa laser 3W, dot per inci (DPI) sebanyak 1200, dan kelajuan laser sehingga 13% telah digunakan bagi mengfabrikasi pengimbas LIG pada substrat Kapton. Pencirian bahan sperti SEM, EDX, dan spektrum Raman dilakukan pada LIG-SPE yang direka bagi mengesahkan kehadiran LIG. Pengukuran voltametri kitaran (CV) dilakukan menggunakan 0.1M $[Fe(CN)_6]^{3-/4-}$ dan 0.1M KCL bagi mencari kadar imbasan yang sesuai. Pada kadar imbasan tetap 50 mV/s, prestasi pengimbas dianalisa menggunakan 0.1M nikotin dengan 3 larutan penimbal fosfat (PBS) berbeza pH 5, pH 7, dan pH 9 pada kepekatan nikotin berbeza. Nikotin dengan larutan PBS pH 5 didapati sebagai larutan optimum, dengan nilai $R^2$ tertinggi 0.9988 dan LOD terendah 4.2183 µM. Kesimpulannya, pengimbas elektrokimia nikotin menggunakan laser elektrod skrin bercetak graphen teraruh dapat mengesan nikotin dengan pemalaran tinggi pada pH larutan penimbal PBS yang berbeza.

***KEYWORDS:*** *laser-induced graphene, screen-printed electrode, nicotine, shrimp virus, electrochemical.*

# 1. INTRODUCTION

Nicotine, a highly addictive substance in tobacco plants, contributes to a global health crisis through smoking addictions. Nicotine poses serious health effects, including respiratory problems, cardiovascular system, and increased risk of lung cancer [1]. Gas chromatography/mass spectrometry (GC-MS), electro-chemiluminescent/flow injection analysis, and high-performance liquid absorption spectrometry (AAS) are among several analytical methods typically used to detect nicotine [2]. Despite providing accurate measurement results, these methods have some drawbacks, such as the need for skilled personnel to conduct the instrument and the fact that they are not portable, making them unsuitable for healthcare monitoring. Hence, there is an urgent need to develop a rapid and portable sensor to detect nicotine in various body fluids such as saliva, sweat, and urine. Electrochemical-based screen-printed electrode (SPE) sensor is regarded as a more suitable sensor for nicotine detection because of its ease of use, cost-effectiveness, and portability [3], [4]. [5]. However, SPE has limitations for electrochemical sensing applications, such as low robustness and limited electrochemical performance compared to conventional electrodes like glassy carbon or golden disk electrodes [1]. One of the drawbacks of glassy carbon electrodes is that they can exhibit a lack of electrochemical inertness under certain conditions, which can lead to the formation of an insulating layer on the surface, particularly when exposed to an oxidative environment; this later significantly reduces the current density and can compromise the electrode's performance over time. On the other hand, gold disk electrodes are susceptible to surface oxidation and can be affected by surface contamination, which may block active sites and hinder the electrochemical reactions [6], [7], [8]. Meanwhile, LIG offers a lot of advantages, where the formation of the porous network structure of LIG results in high conductivity and high specific surface area [9]. Because of its porous nature, the material has more accessibility to chemical processes [10]. Therefore, a laser-induced graphene (LIG) screen-printed electrode is proposed for nicotine detection.

https://doi.org/10.31436/iiumej.v26i1.3392

Graphene structure formation provides the basis for the construction of LIG, a three-dimensional porous carbon-based material constructed on a polyimide substrate [10], [11], [12]. A CO2 infrared laser is utilized to convert polyimide into LIG, which requires high temperatures and pressures. The formation of LIG leads to high electrical conductivity [9] because of graphene's large surface area and inherent superior chemical, physical, and electronic qualities [10]. LIG-based biosensors have been reported to be used in many applications, including glucose detection [13], neurotransmitter detection such as dopamine and serotonin [14], as well as protein and biomarker sensing, including cancer biomarkers, folic acids, and DNA methylation [15]. LIG electrochemical sensors can also be used to detect heavy metal ions, such as aluminum, in soil and water samples [16]. LIG's mechanical flexibility and conformity make it a promising material for fabricating wearable and flexible biosensors, which can be integrated into smart textiles or directly applied to the skin for continuous health monitoring. Recent advancements in nicotine detection have focused on the development of electrochemical sensors, particularly using SPE. However, a modification of SPE is needed to enhance the electrochemical sensing capabilities for nicotine detection. However, there are limited studies on nicotine detection using LIG-SPE sensors. Hence, this work aims to investigate the performance of LIG-SPE sensors in nicotine detection at different pH levels. The paper's organization is as follows: Section 2 explains the design concept of a laser-induced graphene screen-printed electrode. Section 3 discusses the materials and methods for simulating and fabricating laser-induced graphene screen-printed electrodes. Section 4 presents the simulation results, measurements, and performance analysis of electrochemical-based laser-induced graphene screen-printed electrodes for nicotine detection. Finally, the conclusion and future work are discussed in Section 5.

## 2. DESIGN CONCEPT OF ELECTROCHEMICAL-BASED LASER-INDUCED GRAPHENE SCREEN PRINTED ELECTRODE

Graphene is a widely used material in various technologies and is typically synthesized through chemical reduction methods like Hummer's method, which involves oxidizing graphite to graphene oxide before converting it to graphene [17]. Traditional methods like chemical vapor deposition (CVD) are surface-based coating techniques commonly used to produce graphene. However, they can be energy-intensive and have environmental concerns due to chemical treatments and toxic by-products [17]. Meanwhile, a single step of direct laser scribing carbonaceous precursors yields LIG, a three-dimensional carbon-based nanomaterial [18]. LIG offers advantages over traditional graphene synthesis methods as it is cost-effective, swift, and environmentally friendly. It does not require aggressive chemical conditions, extreme temperatures, or vacuum, making it sustainable and efficient [18]. Because it can be molded into numerous 3D forms with high surface-to-volume ratios, LIG may be created from various carbon-containing precursors, such as polyimide, wood, or even food. This makes it appropriate for applications like supercapacitors and sensors. [19]. However, the most common substrate used for LIG formation is polyimide substrate [11], [12], [20]. To obtain a 3D porous graphene structure, photochemical and thermal conversion processes from laser irradiation of a polymeric precursor should occur [12]. Thus, a CO2 infrared laser is used for this purpose [9], [21].

The LIG-SPE sensor consists of four layers, starting from the polyimide substrate, followed by LIG electrodes in Layer 1, Ag electric lines in Layer 2, an AgCl reference electrode in Layer 3, and the final layer, the encapsulation layer, as illustrated in Figure 1. Figure 2 (a) shows the cross-sectional view of the LIG-SPE sensor, while Figure 2 (b) shows the detailed dimensions

https://doi.org/10.31436/iiumej.v26i1.3392

of the design in mm. The working electrode and counter electrode were made using LIG fabrication.

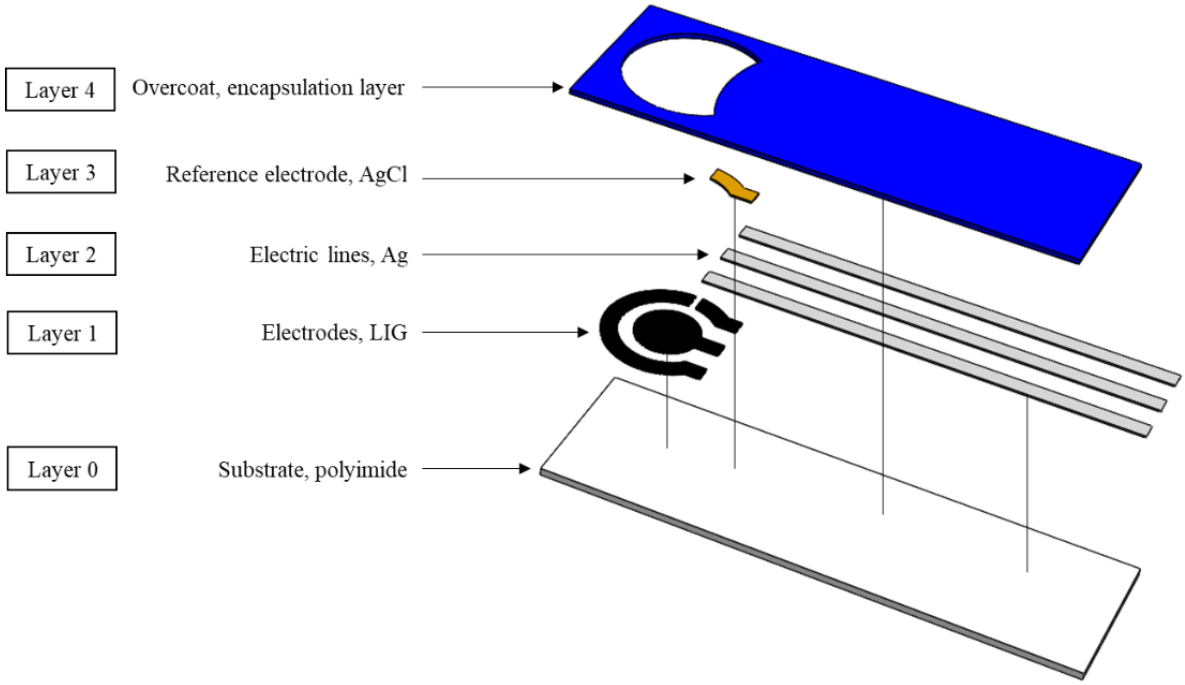


Figure 1. The exploded views of the LIG-SPE design by layers where the working electrode and counter electrode (Layer 1) of the screen-printed electrode were made using LIG fabrication

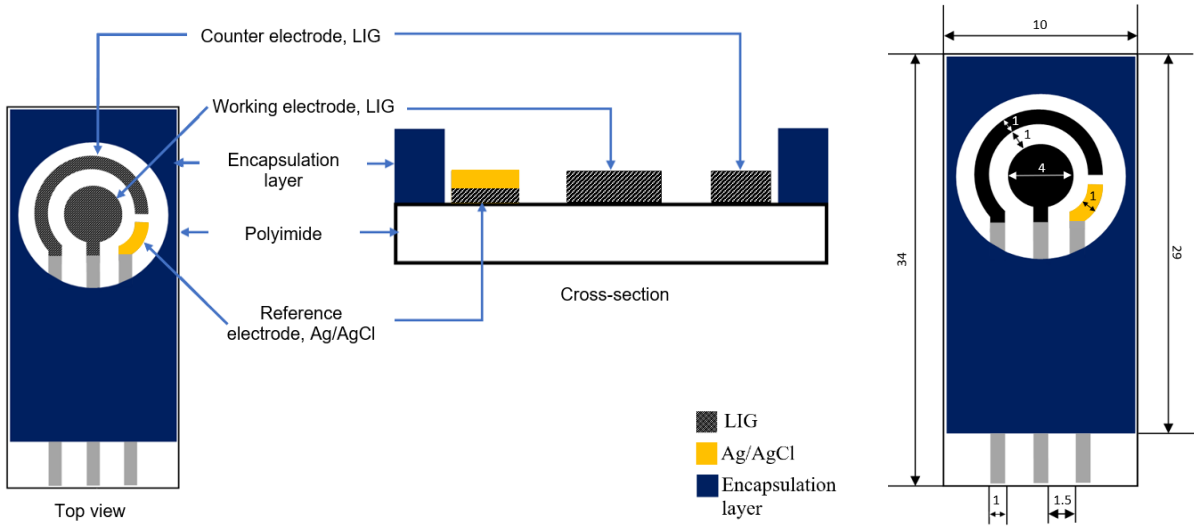


(a) (b)

Figure 2. (a) The cross-section of LIG-SPE showing all layers (b) The dimensions of LIG-SPE in mm

https://doi.org/10.31436/iiumej.v26i1.3392

# 3. MATERIAL AND METHODS

The optimization of laser parameters is vital for LIG fabrication because it determines the quality and properties of the produced graphene. Hence, a finite element simulation was conducted to investigate the effect of laser power on polyimide temperature. The fabrication of LIG-SPE using $CO_2$ laser was later performed with optimal laser parameters.

## 3.1. Finite Element Simulation of Laser Parameters

Numerous variables, including the kind of precursor material, the desired characteristics of the final graphene, and the particular application, contribute to the optimization of laser power. The power required for the LIG process depends on parameters like the material type, the desired graphene quality, the process speed, the laser setup and parameters, and the scale of production [22]. Typically, for the fabrication of LIG, a $CO_2$ laser with powers ranging from a few watts to tens or hundreds of watts is used [23]. The best analytical electrodes were obtained using a 1000 x 1000 CO2 pulse density with a modest, frequent energy input (low laser power) and speed setting. Too much energy input of laser power and laser speed can result in brittle electrodes that would peel off the substrate easily [24]. In the meantime, the substrate was either not carbonized at all or only partially carbonized at high power and speed levels [24].

A finite element simulation is carried out to examine the impact of laser power on the polyimide's temperature. The simulation examined the effect of varying laser power on the polyimide's temperature. The laser strength is adjusted in 1-percent increments between 1% and 5% of 30 W, and the mesh used is in a finer size. Figure 3 (a) shows a circular structure representing the working electrode (WE) of LIG-SPE, while Figure 3(b) shows the mesh of the working electrode with the thickness of the polyimide, 0.1mm.

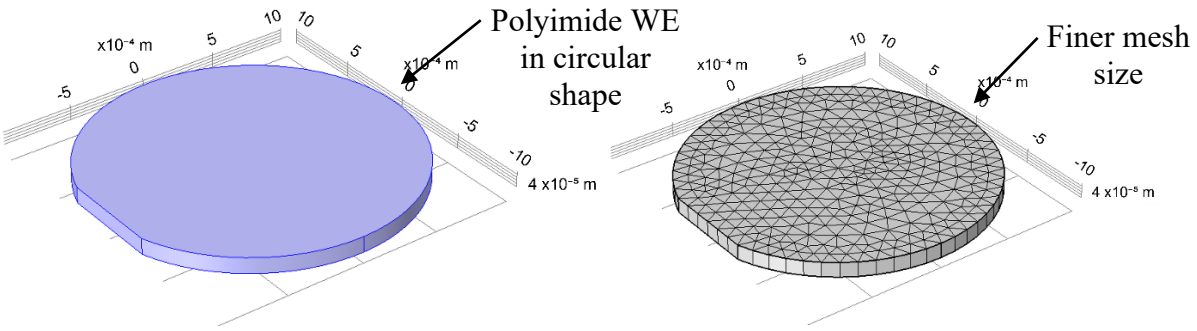


Figure 3. (a) The working electrode (WE) of LIG-SPE
(b) The mesh design of WE uses a finer mesh size

## 3.2. Fabrication of LIG

A $CO_2$ laser is used to fabricate the LIG-SPE sensor because it is good at producing flexible, affordable electrodes on various sustainable and recyclable materials [23]. The $CO_2$ lasers emit infrared light at a wavelength of around 10.6 µm and are known for their high-power output [23]. A CO2 laser's high-power output can produce localized heating on a suitable carbonaceous substrate, like polyimide, which can develop a structure like graphene on the surface of the material [25]. LIG-SPE was fabricated using $CO_2$ laser with laser power parameters 3 W, speed of 13%, and DPI of 1200. The substrate used to produce the LIG-SPE is Kapton or PET. The LIG-SPE consists of four separate layers: LIG serves as the counter and

https://doi.org/10.31436/iiumej.v26i1.3392

working electrode, silver (Ag) serves as a trace, silver-silver chloride (AgCl) serves as the reference electrode, and an encapsulating layer is the last layer. Figure 4(a) depicts the cross-section of the four layers, and Figure 4(b) shows the fabricated LIG-SPE, which was carried out at Jabil Circuit Sdn. Bhd.

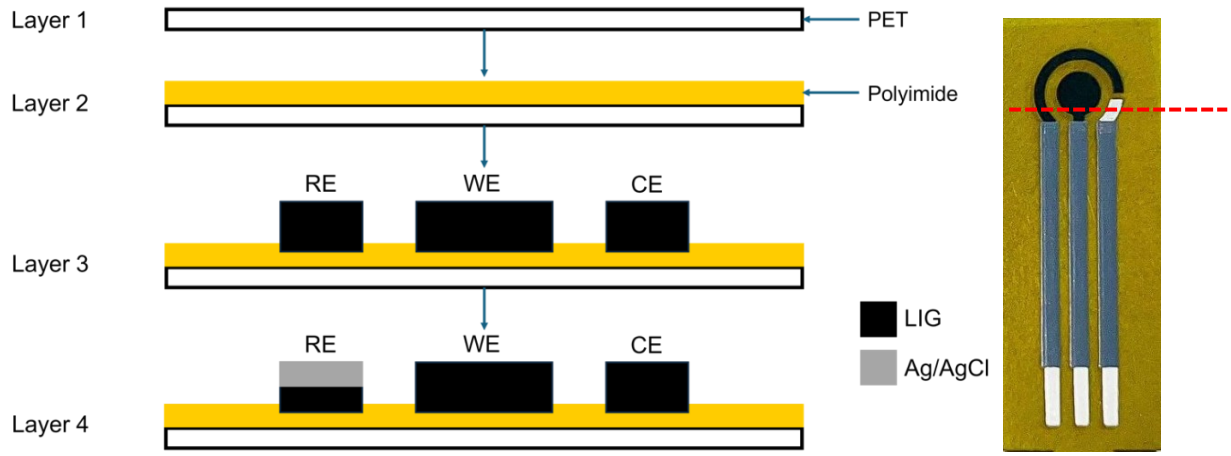


Figure 4. (a) The cross-section view of each layer in the fabrication process of LIG-SPE (b) The fabricated electrode of LIG-SPE

### 3.3. Material Characterization of LIG

Scanning electron microscopy (SEM) was performed to observe the surface morphology of LIG using SEM JEOL JSM-IT100 with an accelerating voltage of 8kV. Energy dispersive X-ray (EDX) integrated with SEM was utilized to provide elemental analysis and chemical characterization of LIG. Raman spectra were analyzed to see the characterization of LIG using the parameters setup of laser power, 1.7 mV, and Raman shift range from 80 $cm^{-1}$ to 3100 $cm^{-1}$.

### 3.4. Experimental Setup for Electrochemical Analysis Performance

Electrochemical testing is carried out to measure the LIG-SPE sensor's performance. Figure 5 illustrates the experimental setup of electrochemical-based LIG-SPE. The LIG-SPE sensor is connected to the PalmSens Emstat Pico Development Kit potentiostat, and electrochemical measurement is analyzed by connecting the potentiostats to the PSTrace software. The measurement set used for the electrochemical analysis performance is a cyclic voltammetry (CV) measurement, starting with the measurement from ferricyanide, [Fe(CN)6]3-/4- and potassium chloride (KCl) solutions to obtain valuable information about the electrochemical behavior of the redox system. A 100 mL of 0.01 M Ferricyanide solution, with 0.1 M of potassium chloride, KCL was prepared for CV measurements at various scan rates from 10 mV/s to 200 mV/s. Once a significant redox peak was shown, the LIG-SPE sensor performance was then tested at various concentrations of nicotine from 20 µM to 100 µM with 3 different phosphate buffer solutions (PBS) of pH-5, pH-7, and pH-9, using CV measurements with scan rate fixed at 50 mV/s.

## 4. RESULTS AND DISCUSSION

This section presents the results and analysis of the simulation and fabrication of LIG-SPE. It also discusses the CV measurements of the fabricated LIG-SPE sensor at various nicotine pH values.

https://doi.org/10.31436/iiumej.v26i1.3392

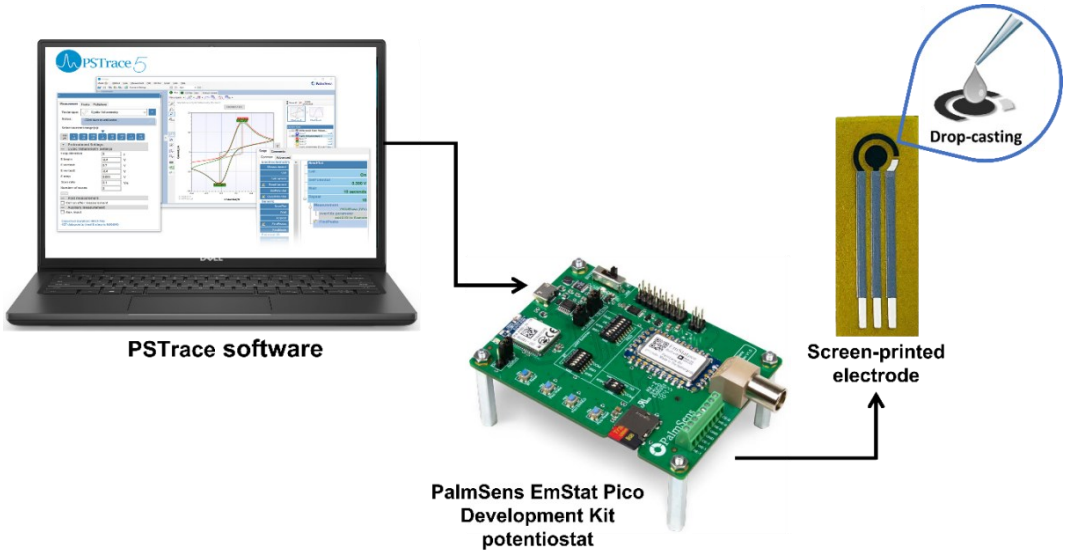


Figure 5. The experimental setup comprises the PalmSens Emstat Pico Development Kit potentiostat, PSTrace software, and a screen-printed electrode.

### 4.1. Simulation Results on the Effect of Laser Parameters for LIG

A laser power in the range of 1% to 5% of 30 W was studied using finite element simulation to investigate its effects on the temperature of polyimide substrate. Figure 6 shows the graph of the polyimide's temperature against time when a laser is fired onto the substrate. The graph shows that the laser power of 1% is the most stable, as the temperature is steadily rising, unlike the other laser powers, which are increasing rapidly. When the laser power increases, the temperature of polyimide also increases. However, a temperature that is too high can destroy the polyimide's surface, affecting the quality of the LIG electrode. A brittle electrode would readily peel off the substrate when the temperature is too high and when there is excessive energy input [26]. Figure 7 (a) shows the temperature of the polyimide substrate when the laser beam was irradiated onto the substrate, showing the heating profile on the surface with the highest temperature observed at the center. Figure 7 (b) shows the thermal contour of the polyimide when the laser beam was irradiated, indicating the temperature was distributed through the substrate thickness. This shows the laser's capability to heat the polyimide substrate to induce graphene at a laser power of 1%.

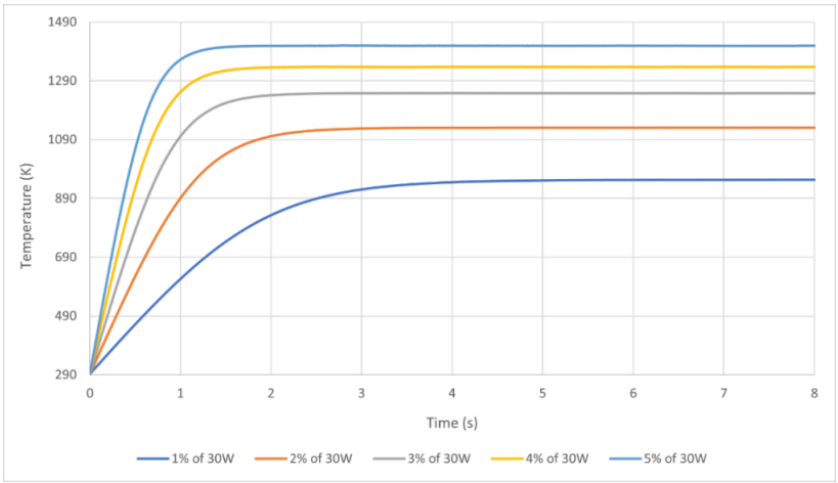


Figure 6. Graph of temperature of polyimide versus time based on the different laser powers (1%, 2%, 3%, 4%, and 5% of 30 W)

https://doi.org/10.31436/iiumej.v26i1.3392

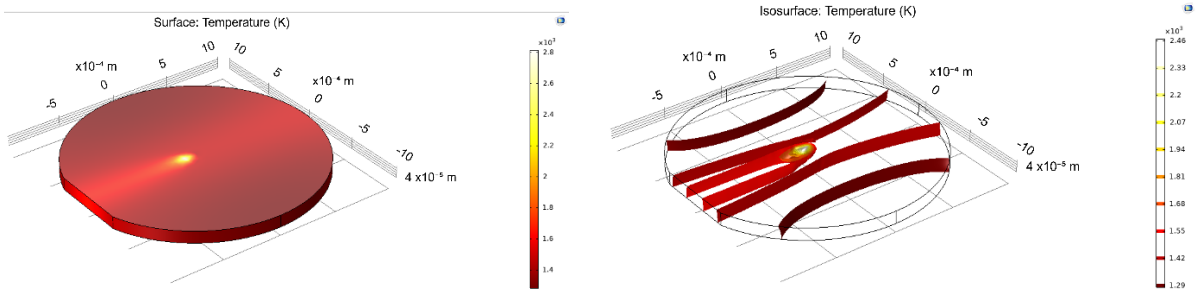


(a) (b)

Figure 7. (a) The temperature of the polyimide (b) The thermal contour of the polyimide

### 4.2. Material Characterization of LIG

After LIG-SPE was fabricated, material characterizations were carried out to confirm the formation of LIG on the polyimide substrate. Figure 8 (a) shows the SEM image of the LIG-SPE cross-section displaying two distinct layers of LIG (thickness of 176.018 µm) and polyimide (thickness of 142.004 µm). Figures 8 (b) and (c) display the SEM images of LIG-SPE with a porous structure, which can be clearly visible at 1k and 3k magnifications, respectively.

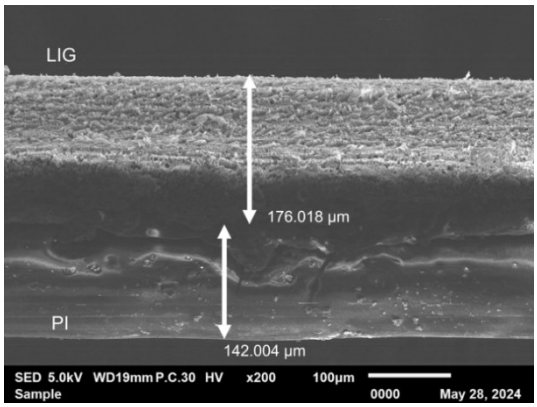


(a)

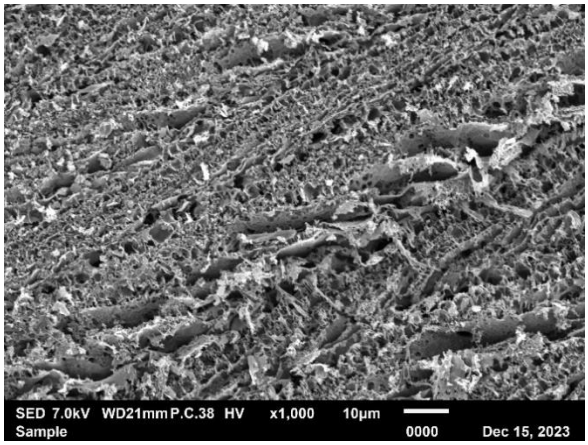


(b)

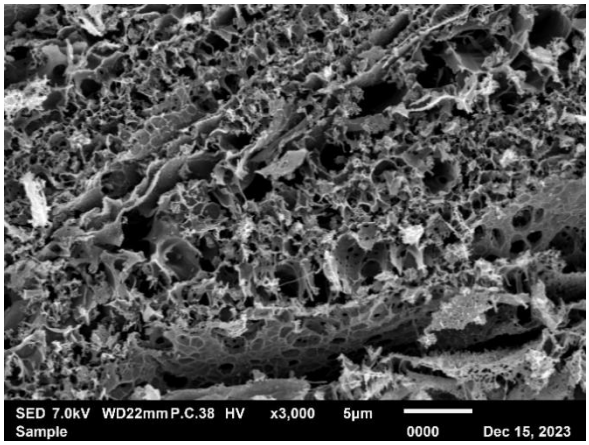


(c)

Figure 8. (a) SEM image of LIG-SPE cross-section (b) SEM images of LIG-SPE showing the porous structure at 1k magnification (c) at 3k magnification

https://doi.org/10.31436/iiumej.v26i1.3392

The LIG porous structure is similar to the surface morphology results reported by Kim et al. [27]. Due to a carbon network resembling graphene, LIG's porous structure allows for an extremely large surface area-to-volume ratio [16]. This property renders LIG electrically conductive [9]. EDX spectra of LIG that can be seen in Figure 9 show strong peaks corresponding to carbon (C) and oxygen (O), indicating the presence of graphene-based structure via laser irradiation. Table 1 presents the map sum spectrum of C and O weight percentage values for LIG, which conforms to the compositions described in [32], [33].

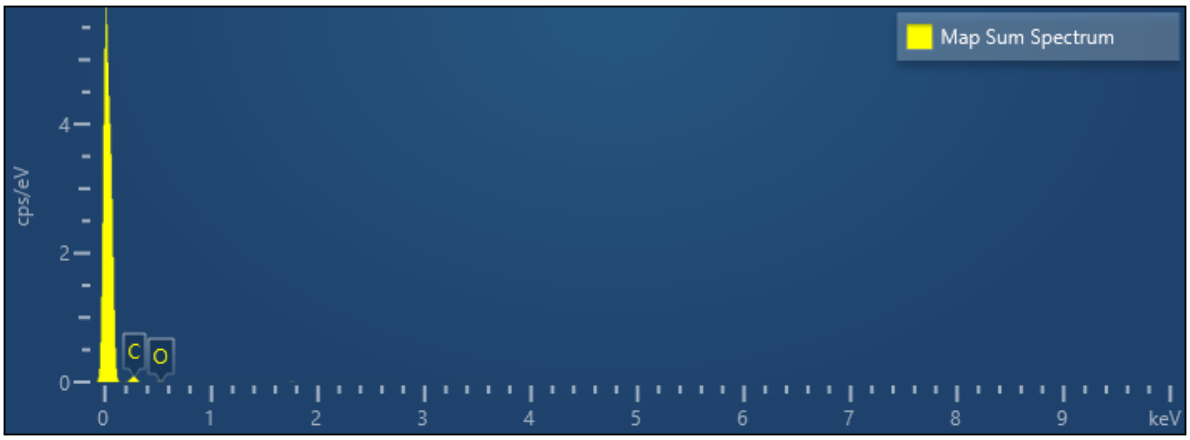


Figure 9. The map sum spectrum of LIG showing carbon (C) and oxygen (O) peaks

Table 1. Map sum spectrum of LIG-SPE

| Element | Line Type | Weight % | Weight % Sigma | Atomic % |
|---|---|---|---|---|
| **C** | K series | 90.31 | 2.78 | 92.55 |
| **O** | K series | 9.69 | 2.78 | 7.45 |
| **Total** | | 100.00 | | 100.00 |

The analysis of Raman spectra is important to analyze the presence of graphene in LIG-SPE. Three principal peaks are typically observed for graphene: the D peak at 1308 $cm^{-1}$, the G peak at 1595 $cm^{-1}$, and the 2D peak at 2612 $cm^{-1}$, as shown in Figure 10. These peaks correspond well with the peaks of ~1330 $cm^{-1}$ (D peak), ~1580 $cm^{-1}$ (G peak), and ~2660 $cm^{-1}$ (2D peak) as reported in [28].

### 4.3. Electrochemical Measurement

The electrochemical measurement was conducted to evaluate the LIG-SPE sensor's performance in nicotine detection. A CV measurement of 0.01 M [Fe(CN)6]3-/4- with 0.1 M KCL at various scan rates from 10 mV/s to 200 mV/s was carried out to observe the redox peak on the LIG-SPE sensor. The CV measurement was then continued to check the sensor's performance by using various nicotine concentrations from 20 µM to 100 µM with 3 different phosphate buffer solutions (PBS) of pH 5, pH 7, and pH 9 at a fixed scan rate of 50 mV/s.

https://doi.org/10.31436/iiumej.v26i1.3392

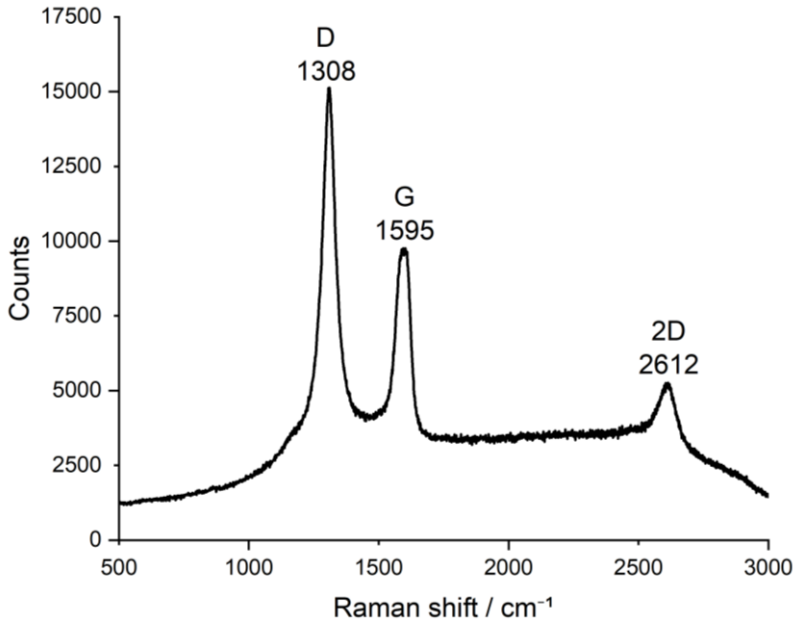


Figure 10. Raman spectroscopy of the LIG-SPE displaying the graphene D, G, and 2D peaks

### *4.3.1. Effect of Different Scan Rates*

Cyclic voltammetry (CV) is an electroanalytical technique used to study the electrochemical properties of a system by applying a linearly varying potential to an electrode immersed in an electrolyte solution and measuring the resulting current [29]. Increasing the scan rate can make an irreversible system appear more reversible by competing with the timescale of the follow-up chemical reaction [29]. At very slow scan rates, an irreversible system may show no peaks at all, while at faster scan rates, the peaks become more pronounced [29]. The CV measurements of LIG-SPE were performed using 0.1 M ferricyanide and 0.1 M KCL at various scan rates from 10 mV/s to 200 mV/s. The values from the LIG-SPE sensor at different scan rates are displayed in Figure 11. The graph shows distinct oxidation and reduction peaks, indicating that the anodic and cathodic currents increase with the scan rates.

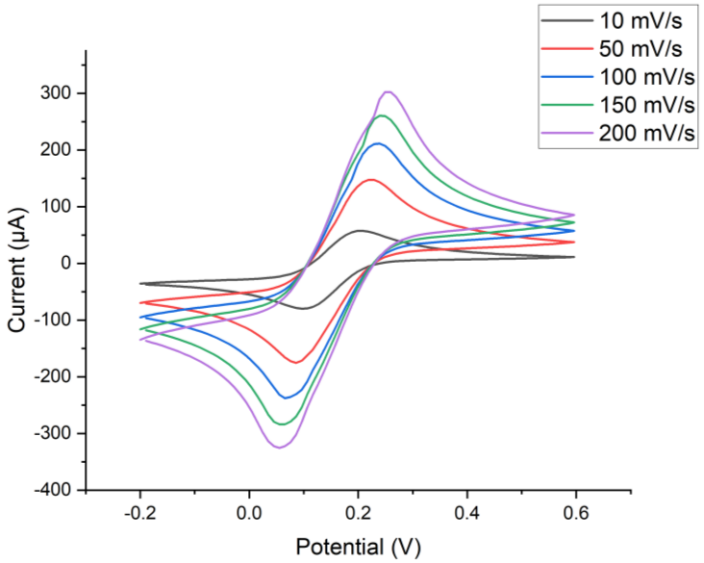


Figure 11. CV measurements for LIG-SPE at various scan rates from 10 mV/s to 200 mV/s

https://doi.org/10.31436/iiumej.v26i1.3392

### *4.3.2. Effect of Different pH Values on Nicotine Detection*

CV measurements were performed using different nicotine concentrations ranging from 20 µM to 100 µM with three different PBS pH values: pH 5, pH 7, and pH 9 at a fixed scan rate of 50 mV/s. Figure 16 displays the CV readings obtained by the LIG-SPE sensor at different nicotine concentrations for PBS pH 5, pH 7, and pH 9. In general, it can be observed that LIG-SPE can effectively detect nicotine in a PBS solution with the maximum oxidation peak at the highest concentration of 100 µM. Figure 12 shows the graph of the oxidation peak versus nicotine concentration for PBS at pH 5, pH 7, and pH 9. The calibration curve, $R^2$, and limit of detection, LOD for pH 5 are 0.9988 and 4.2183 µM. For pH 7, the values are 0.9912 and 11.3892 µM; for pH 9, the R2 and LOD values are 0.998 and 5.43399 µM, respectively. To determine how well the calibration curve value, $R^2$ was established, $R^2$ values above 0.990 generally indicate that calculated unknown values will be close to accurate across the calibration curve [30]. These values are summarized in Table 2.

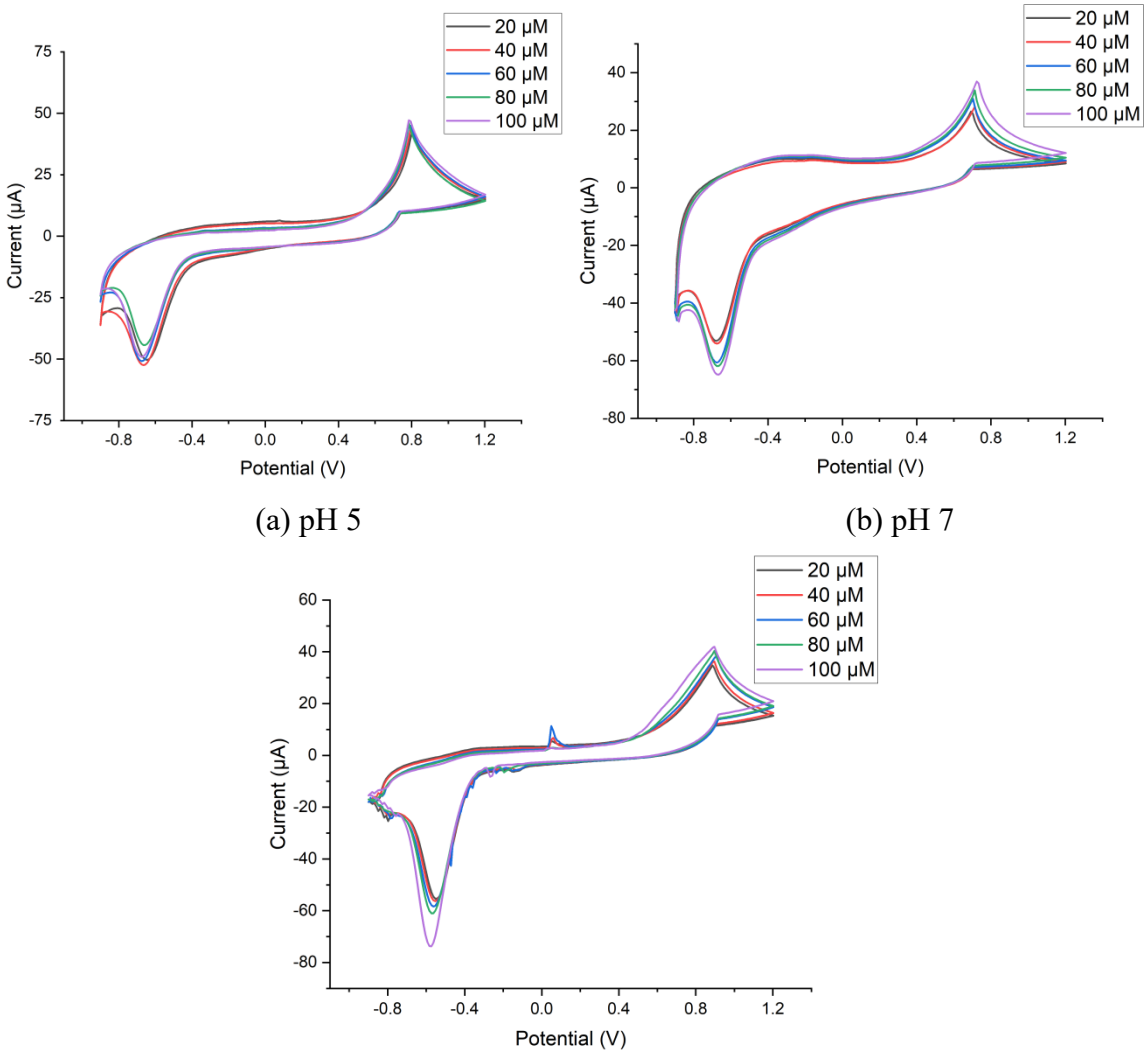


(a) pH 5

(b) pH 7

(c) pH 9

Figure 12. Current vs. potential graph of different concentrations of nicotine for (a) PBS pH 5, (b) pH 7, and (c) pH 9

https://doi.org/10.31436/iiumej.v26i1.3392

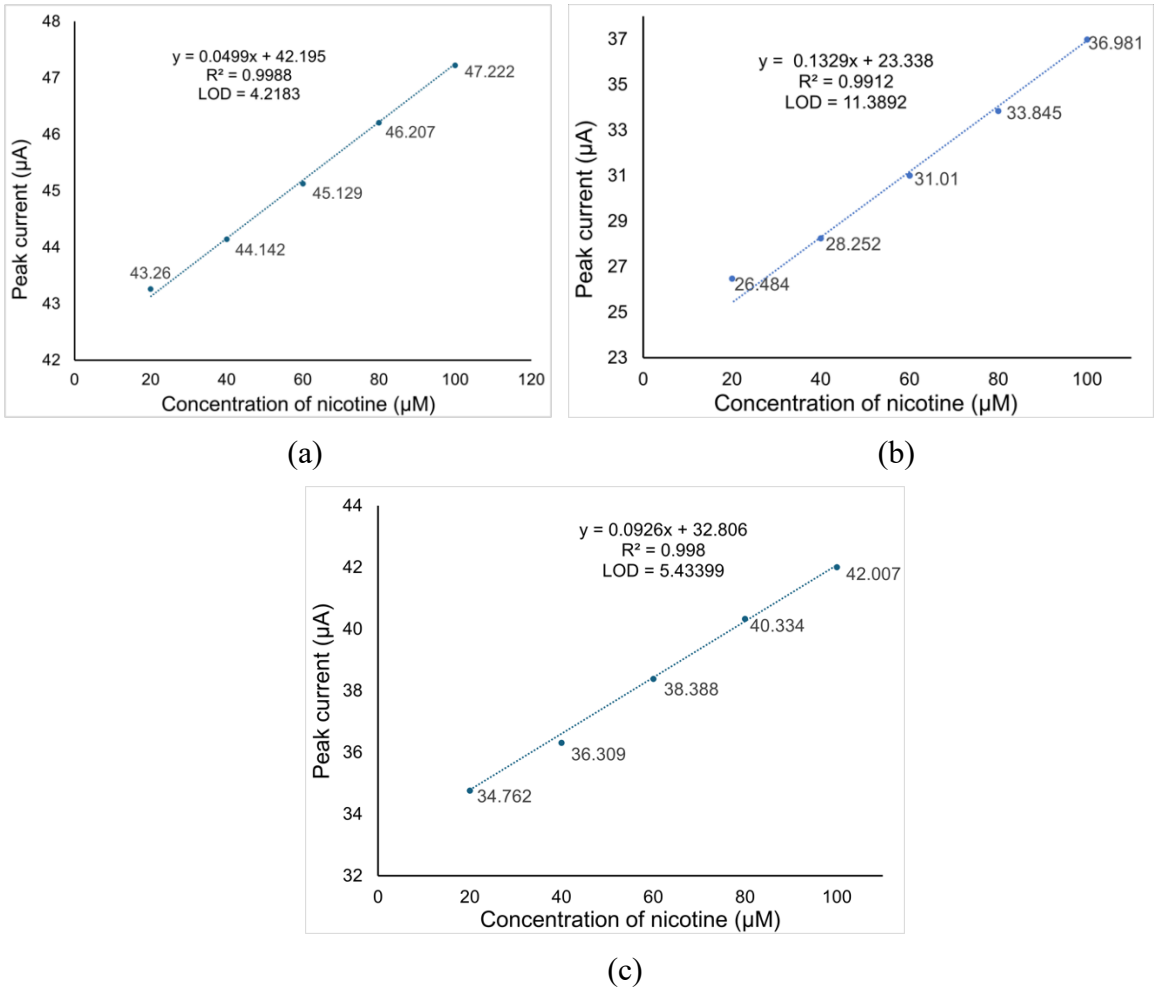


Figure 13. Oxidation peak vs. concentration of nicotine for PBS at (a) pH 5, (b) pH 7, and (c) pH 9

Table 2. Value of $R^2$ and LOD at different pH values

| pH value for PBS | $R^2$ | LOD (μM) |
|---|---|---|
| pH 5 | 0.9988 | 4.2183 |
| pH 7 | 0.9912 | 11.3892 |
| pH 9 | 0.9980 | 5.43399 |

Table 2 shows the values of the LIG-SPE's calibration curve, $R^2$, and LOD on detecting nicotine at different pH values. Based on the table shows that nicotine at pH 5 has the highest $R^2$ value of 0.9988 and the lowest LOD of 4.22 μM. This observation can be explained by considering that most sensors efficiently detect the predominant species of monoprotonated nicotine ions. Because nicotine is a weak base, its presence in the environment might cause it to ionize or non-ionize [31], [32]. Nicotine is mainly ionized in acidic environments and predominantly in its unionized form in alkaline environments [33]. At pH levels below 3, the predominant species is the diprotonated nicotinium ion ($NicH^{2+}$), where nicotine has gained 2 extra protons, resulting in doubly positively charged species [33]. The sensor does not efficiently sense diprotonated nicotine, as the potential decreases due to the formation of the species at low pH levels. However, at pH levels between 3.5 and 6.5, the predominant species is the monoprotonated nicotine ion ($NicH^{+}$), where nicotine has gained one extra proton,

resulting in a positively charged species efficiently sensed by most sensors [33]. Hence, sensors display optimal sensitivity within this pH range. As for the above pH 7, the predominant species is the non-protonated nicotine base, which is not associated with any additional protons, making it electrically neutral [33]. Nicotine is not ionized and does not carry a charge. Consequently, the LIG-SPE sensor shows lower sensitivity at higher pH levels. Table 3 summarizes the performance of LIG-SPE for nicotine sensors and comparison with previous works. This work contributes to the LIG-SPE's ability to detect nicotine without surface modification with good linearity and low detection limits.

Table 3. Summary of the performance of LIG-SPE for nicotine sensor and comparison with other previous works

| Type of sensor | Surface modification | $R^2$ | LOD | Ref |
|---|---|---|---|---|
| **SPCE** | β-CB grafted | * | 50.80 µM | [34] |
| | FC-MWCNTs | * | 4.25 µM | [35] |
| | AuNPs | 0.9920 | 8.30 mM | [36] |
| **LIG-SPE** | - | 0.9988 | 4.22 µM | This work (at pH 5 PBS solution) |

* Not specified

## 5. CONCLUSION

In summary, we have demonstrated the simulation and fabrication of laser-induced graphene screen-printed electrodes for nicotine detection. The finite element simulation result shows that the laser power of 1% is the most stable, as the temperature is steadily rising, unlike the other laser powers, which are increasing rapidly. When the laser power increases, the temperature of polyimide also increases. LIG fabrication was performed at the working and counter electrode of LIG-SPE using the optimum laser power based on the simulation results. Based on the electrochemical measurements, nicotine with PBS pH 5 solution was found to yield the optimum result, with the value obtained for the calibration curve. The $R^2$ value was the highest at 0.9988, and the LOD value of 4.2183 among all. Therefore, laser-induced graphene (LIG) electrochemical sensors show great potential for detecting nicotine.

## ACKNOWLEDGEMENT

This work is fully supported by the Ministry of Higher Education (MOHE) Fundamental Research Grant Scheme FRGS21-239-0848 (FRGS/1/2021/TK0/UIAM/02/9).

## REFERENCES

[1] A. García-Miranda Ferrari, S. J. Rowley-Neale, and C. E. Banks, "Screen-printed electrodes: Transitioning the laboratory in-to-the field," Aug. 01, 2021, *Elsevier B.V.* doi: 10.1016/j.talo.2021.100032.

[2] E. Mehmeti, T. Kilic, C. Laur, and S. Carrara, "Electrochemical determination of nicotine in smokers' sweat," *Microchemical Journal*, vol. 158, p. 105155, Nov. 2020, doi: 10.1016/J.MICROC.2020.105155.

[3] A. Hayat and J. L. Marty, "Disposable screen printed electrochemical sensors: Tools for environmental monitoring," Jun. 13, 2014, *MDPI AG*. doi: 10.3390/s140610432.

[4] Z. Taleat, A. Khoshroo, and M. Mazloum-Ardakani, "Screen-printed electrodes for biosensing: A review (2008-2013)," 2014, *Springer-Verlag Wien*. doi: 10.1007/s00604-014-1181-1.
[5] A. V. Shokurov and C. Menon, "Laser-Induced Graphene Electrodes for Electrochemistry Education and Research," *J Chem Educ*, Jun. 2022, doi: 10.1021/acs.jchemed.2c01237.
[6] S. Michalkiewicz, A. Skorupa, and M. Jakubczyk, "Carbon Materials in Electroanalysis of Preservatives: A Review.," *Materials (Basel)*, vol. 14, no. 24, Dec. 2021, doi: 10.3390/ma14247630.
[7] M. Zamani, C. M. Klapperich, and A. L. Furst, "Recent advances in gold electrode fabrication for low-resource setting biosensing.," *Lab Chip*, vol. 23, no. 5, pp. 1410–1419, Mar. 2023, doi: 10.1039/d2lc00552b.
[8] J. Edgington, A. Deberghes, and L. C. Seitz, "Glassy Carbon Substrate Oxidation Effects on Electrode Stability for Oxygen Evolution Reaction Catalysis Stability Benchmarking," *ACS Appl Energy Mater*, vol. 5, no. 10, pp. 12206–12218, Oct. 2022, doi: 10.1021/acsaem.2c01690.
[9] J. Lin *et al.*, "Laser-induced porous graphene films from commercial polymers," *Nat Commun*, vol. 5, 2014, doi: 10.1038/ncomms6714.
[10] L. Huang, J. Su, Y. Song, and R. Ye, "Laser-Induced Graphene: En Route to Smart Sensing," Aug. 01, 2020, *Springer*. doi: 10.1007/s40820-020-00496-0.
[11] A. R. Cardoso *et al.*, "Molecularly-imprinted chloramphenicol sensor with laser-induced graphene electrodes," *Biosens Bioelectron*, vol. 124–125, pp. 167–175, Jan. 2019, doi: 10.1016/j.bios.2018.10.015.
[12] F. M. Vivaldi *et al.*, "Three-Dimensional (3D) Laser-Induced Graphene: Structure, Properties, and Application to Chemical Sensing," Jul. 07, 2021, *American Chemical Society*. doi: 10.1021/acsami.1c05614.
[13] K. Y. Lau and J. Qiu, "Broad applications of sensors based on laser-scribed graphene," *Light Sci Appl*, vol. 12, no. 1, p. 168, Jul. 2023, doi: 10.1038/s41377-023-01210-6.
[14] Y. Guo, C. Zhang, Y. Chen, and Z. Nie, "Research Progress on the Preparation and Applications of Laser-Induced Graphene Technology.," *Nanomaterials (Basel)*, vol. 12, no. 14, Jul. 2022, doi: 10.3390/nano12142336.
[15] G. Bhattacharya *et al.*, "Disposable Paper-Based Biosensors: Optimizing the Electrochemical Properties of Laser-Induced Graphene," *ACS Appl Mater Interfaces*, vol. 14, no. 27, pp. 31109–31120, Jul. 2022, doi: 10.1021/acsami.2c06350.
[16] Z. Wan, N. T. Nguyen, Y. Gao, and Q. Li, "Laser induced graphene for biosensors," Sep. 01, 2020, *Elsevier B.V.* doi: 10.1016/j.susmat.2020.e00205.
[17] N. Dixit and S. P. Singh, "Laser-Induced Graphene (LIG) as a Smart and Sustainable Material to Restrain Pandemics and Endemics: A Perspective," *ACS Omega*, vol. 7, no. 6, pp. 5112–5130, Feb. 2022, doi: 10.1021/acsomega.1c06093.
[18] A. Velasco, Y. K. Ryu, A. Hamada, A. de Andrés, F. Calle, and J. Martinez, "Laser-Induced Graphene Microsupercapacitors: Structure, Quality, and Performance," *Nanomaterials*, vol. 13, no. 5, Mar. 2023, doi: 10.3390/nano13050788.
[19] W. Ma, J. Zhu, Z. Wang, W. Song, and G. Cao, "Recent advances in preparation and application of laser-induced graphene in energy storage devices," Dec. 01, 2020, *Elsevier Ltd*. doi: 10.1016/j.mtener.2020.100569.
[20] R. Ye, D. K. James, and J. M. Tour, "Laser-Induced Graphene: From Discovery to Translation," Jan. 04, 2019, *Wiley-VCH Verlag*. doi: 10.1002/adma.201803621.
[21] R. Ye, D. K. James, and J. M. Tour, "Laser-Induced Graphene," *Acc Chem Res*, vol. 51, no. 7, pp. 1609–1620, Jul. 2018, doi: 10.1021/acs.accounts.8b00084.
[22] M. Fan *et al.*, "CO2 Laser-Induced Graphene with an Appropriate Oxygen Species as an Efficient Electrocatalyst for Hydrogen Peroxide Synthesis," *Chemistry*, vol. 28, no. 60, Oct. 2022, doi: 10.1002/CHEM.202201996.
[23] T. Pinheiro *et al.*, "Influence of CO2 laser beam modelling on electronic and electrochemical properties of paper-based laser-induced graphene for disposable pH electrochemical sensors," *Carbon Trends*, vol. 11, Jun. 2023, doi: 10.1016/j.cartre.2023.100271.

[24] A. Behrent, C. Griesche, P. Sippel, and A. J. Baeumner, "Process-property correlations in laser-induced graphene electrodes for electrochemical sensing," *Microchimica Acta*, vol. 188, no. 5, May 2021, doi: 10.1007/s00604-021-04792-3.
[25] M. Liu, J. N. Wu, and H. Y. Cheng, "Effects of laser processing parameters on properties of laser-induced graphene by irradiating CO2 laser on polyimide," *Sci China Technol Sci*, vol. 65, no. 1, pp. 41–52, Jan. 2022, doi: 10.1007/s11431-021-1918-8.
[26] A. Behrent, C. Griesche, P. Sippel, and A. J. Baeumner, "Process-property correlations in laser-induced graphene electrodes for electrochemical sensing," *Microchimica Acta*, vol. 188, no. 5, May 2021, doi: 10.1007/s00604-021-04792-3.
[27] Y. Il Kim, M. K. Ro, U. Y. Paek, M. K. Sok, and H. Pak, "Maximum Temperature Determination for Stable Operation of Direct-Write Laser-Induced Graphene Heater on Exposed Polyimide Substrate through Numerical Simulation." [Online]. Available: https://ssrn.com/abstract=4254595
[28] J. H. Han, S. Hyun Park, S. Kim, and J. Jungho Pak, "A performance improvement of enzyme-based electrochemical lactate sensor fabricated by electroplating novel PdCu mediator on a laser induced graphene electrode," *Bioelectrochemistry*, vol. 148, Dec. 2022, doi: 10.1016/j.bioelechem.2022.108259.
[29] N. Elgrishi, K. J. Rountree, B. D. McCarthy, E. S. Rountree, T. T. Eisenhart, and J. L. Dempsey, "A Practical Beginner's Guide to Cyclic Voltammetry," *J Chem Educ*, vol. 95, no. 2, pp. 197–206, Feb. 2018, doi: 10.1021/acs.jchemed.7b00361.
[30] "Calibration Part II – Evaluating Your Curves - Cannabis Industry Journal." Accessed: Jun. 22, 2023. [Online]. Available: https://cannabisindustryjournal.com/column/calibration-part-ii-evaluating-your-curves/
[31] S. L. Tomar and J. E. Henningfield, "Review of the evidence that pH is a determinant of nicotine dosage from oral use of smokeless tobacco.," *Tob Control*, vol. 6, no. 3, pp. 219–25, Sep. 1997, doi: 10.1136/tc.6.3.219.
[32] O. Alharbi, Y. Xu, and R. Goodacre, "Simultaneous multiplexed quantification of nicotine and its metabolites using surface enhanced Raman scattering," *Analyst*, vol. 139, no. 19, pp. 4820–4827, Aug. 2014, doi: 10.1039/C4AN00879K.
[33] A. E. G. E. Amr, A. H. Kamel, A. A. Almehizia, A. Y. A. Sayed, E. A. Elsayed, and H. S. M. Abd-Rabboh, "Paper-Based Potentiometric Sensors for Nicotine Determination in Smokers' Sweat," *ACS Omega*, vol. 6, no. 17, pp. 11340–11347, May 2021, doi: 10.1021/acsomega.1c00301.
[34] S. K. Ali *et al.*, "Determination of Caffeic acid in Cigarette Smoke and Urine by Electrochemical Methods Using Supramolecular Electroactive Materials grafted in Screen Printed Carbon Electrode," *Oriental Journal Of Chemistry*, vol. 39, no. 6, pp. 1461–1468, Dec. 2023, doi: 10.13005/ojc/390606.
[35] Z. Su *et al.*, "A smart portable electrochemical sensor based on electrodeposited ferrocene-functionalized multiwalled carbon nanotubes for *in vitro* and *in vivo* detection of nicotine in tobacco samples," *New Journal of Chemistry*, vol. 48, no. 8, pp. 3370–3380, Feb. 2024, doi: 10.1039/D3NJ05035A.
[36] A. Aiman Ali Amran *et al.*, "Gold Nanoparticle Deposited on Screen-Printed Carbon Electrode for Electrochemical Detection of Nicotine in E-cigarette," 2023.